

# FURTHER STUDIES ON THERMAL STABILITY OF MODIFIED 718 ALLOYS

Encai Guo, Fengqin Xu and E.A. Loria

Central Iron and Steel Research Institute  
Beijing, China

and

Niobium Products Company  
Pittsburgh, PA, USA

## Abstract

Continuing the effort to redesign Alloy 718 in order to provide microstructural and mechanical stability beyond 650°C, three modified compositions were studied after appropriate heat treatments. These alloys have demonstrated better thermal stability than conventional Alloy 718 at and above 650°C. In this study, emphasis was placed on the relative stability of the alloy having a non-compact  $\gamma'/\gamma''$  precipitate structure compared to the one having the cube-shaped, compact  $\gamma'/\gamma''$  precipitate structure when aged for 500 and 1000 hr at 700°C. Tensile tests at ambient and at 700°C and stress rupture testing at 700°C under 638 MPa (92.5 ksi) were conducted both before and after these exposures. Better results were obtained with the non-compact precipitate  $\gamma'/\gamma''$  morphology and attributed to a lower coarsening (growth) rate of the  $\gamma'$  and  $\gamma''$  phases for these thermal and stress-enhanced conditions. It should be recognized that this alloy had a W addition to provide increased strength and a slower rate of  $\gamma''$  coarsening. The third alloy changed from a cube-shaped  $\gamma'/\gamma''$  morphology to a mixture of basically non-compact  $\gamma'/\gamma''$  precipitate after the thermal treatments and ranked below the two major emphasis alloys.

## Introduction

This paper is the latest in our series of papers<sup>1-5</sup> whose goal has been to develop a modified Alloy 718 compositions which extends not only the service range to a higher temperature but also improves properties at the present ceiling temperature of 650°C for conventional Alloy 718. The subject has been an active one as shown by recent papers.<sup>6-13</sup> In addition to decreasing the amount of  $\delta$  phase that forms during extended exposure (aging) at and above 650°C, alloy improvement has been focussed on increasing the stability of the  $\gamma'$  and/or  $\gamma''$  phases. Minor modification of the composition via changes in the amounts of the hardening elements coupled with an appropriate heat treatment has provided better thermal stability properties. This has been demonstrated for both the conventional non-compact  $\gamma'/\gamma''$  precipitate morphology<sup>1-9</sup> and the compact  $\gamma'/\gamma''$  cuboidal

precipitate morphology.<sup>10-12</sup> In our prior study,<sup>1</sup> three alloys were compared on the basis of microstructure and mechanical properties and it was found that our Alloy 5 having a non-compact  $\gamma'/\gamma''$  precipitate structure was superior to Alloy 7 which is Andrieu's preferred composition for producing the cube-shaped  $\gamma'/\gamma''$  precipitate.<sup>10</sup> This study presents additional results on this comparison using Andrieu's<sup>11</sup> new heat treatment that produces better results for the compact  $\gamma'/\gamma''$  precipitate structure in Alloy 7.

### Materials and Procedure

The modifications of Alloy 718 were vacuum induction melted and cast as 23 kg ingots in the case of Alloys 5 and 7 and 5 kg ingot in the case of Alloy 3. After homogenizing for 24 hours at 1100°C and for 1 hour at 1160°C to minimize segregation effects, the ingots were hot forged into 32mm bars. Specimens cut from the bars provided the compositions listed in Table I.

Table I Chemical Composition of Alloys									wt. %
Alloy	C	Cr	Mo	Ti	Al	Nb	Fe	W	B
3	0.056	17.58	2.85	0.97	0.86	5.51	17.00		0.0033
5	0.048	16.60	3.09	0.98	0.93	5.57	13.71	2.30	0.0019
7	0.059	17.20	2.98	1.20	1.19	4.95	19.23		0.0041
Alloy	Ti	Al	Nb	Al+Ti+Nb	Al/Ti	Al+Ti/Nb			
3	1.18	1.85	3.44	6.47	1.57	0.88			
5	1.21	2.04	3.55	6.80	1.69	0.92			
7	1.48	2.33	3.16	6.97	1.57	1.21			

As selected from the introductory paper,<sup>1</sup> Alloy 5 was solution treated at 1030°C for 1 hr, air cool, 800°C for 1 hr, then furnace cool (50°/hr) to 650°C, hold for 16 hr and air cool. Alloy 7 was given the new heat treatment of 1025°C for 30 min, air cool, 850°C for 30 min, then furnace cool (200°C/hr) to 650°C, hold for 16 hr and air cool. Alloy 3 was solution treated at 980°C for 1 hr, air cool, 850°C for 1 hr, then furnace cool (50°C/hr) to 650°C, hold 16 hr and air cool. This is the same as the prior heat treatment and the one employed on Alloy 7 in the prior study. These heat treatments produced a  $\gamma$  matrix grain size of ASTM 5-6 for all three alloys. The metallography, tensile and stress rupture testing was done on the heat treated bar stock and after 500 and 1000 hr exposure (aging) at 700°C and followed the standard procedure in each case.

### Results

#### Mechanical Property Evaluation

The results of room temperature and 700°C (1300°F) tensile testing are listed in Tables II to IV together with stress rupture tests at 700°C under a stress of 638 MPa (92.5 ksi). As expected, after 700°C exposure, the yield and ultimate strength declined in each alloy, with notable differences between Alloys 5 and 7. Also, it should be recognized that the values for all three alloys are significantly higher than the 862 MPa (125 ksi) yield strength and 937 MPa (136 ksi) ultimate strength obtained on current Alloy 718 at 700°C, per K-M Chang.<sup>14</sup> In regard to ductility, the elongation and reduction of area values either improved or remained essentially the same with holding time at 700°C, with all tests producing acceptable results. Finally, it

Table II Mechanical Properties of Alloy 5 after Specified Heat Treatment

Heat Treat	Tensile Test Results					Stress Rupture Test Results				
	Temp °C	Yield MPa	Ult MPa	El %	RA %	Temp °C	Stress MPa	Time hr	El %	RA %
A	25	1110	1485	22.3	36.6	700	638	30.4	6.4	11.2
	25	1120	1460	21.0	33.7	700	638	52.9	10.8	19.0
	700	925	1140	9.9	16.1	700	638	31.8	8.2	18.3
B	25	1065	1485	17.5	31.5	700	638	44.0	19.0	24.2
	25	1180	1510	19.0	31.5	700	638	45.1	22.1	31.7
	700	1020	1140	32.0	31.5	700	638			
	700	1035	1170	29.0	37.5	700	638			
C	25	1180	1515	16.5	28.5	700	638	32.2	11.8	25.5
	25	1200	1525	16.0	26.5	700	638	45.0	14.4	23.0
	700	1035	1170	25.5	53.5					
	700	1015	1150	24.5	39.0					

A = As heat treated      B = A + 700°C, 500 hr      C = A + 700°C, 1000 hr

Table III Mechanical Properties of Alloy 7 after Specified Heat Treatment

Heat Treat	Tensile Test Results					Stress Rupture Test Results				
	Temp °C	Yield MPa	Ult MPa	El %	RA %	Temp °C	Stress MPa	Time hr	El %	RA %
A	25	1050	1470	20.0	29.0	700	638	23.6	3.7	7.4
	25	1085	1485	21.0	29.5	700	638	26.5	9.4	9.7
	700	895	1105	10.0	14.0					
B	700	905	1125	11.0	15.0					
	25	1070	1465	18.0	33.0	700	638	33.3	14.9	15.4
	25	1060	1480	17.5	32.5	700	638	27.3	13.7	21.0
	700	995	1130	28.5	35.5					
C	700	965	1120	21.0	43.5					
	25	1085	1490	17.5	29.5	700	638	26.0	14.2	20.7
	25	1100	1475	17.0	28.0	700	638	18.0	9.4	22.3
	700	975	1090	23.5	30.5					
	700	975	1095	29.0	41.0					

A = As heat treated      B = A + 700°C, 500 hr      C = A + 700°C, 1000 hr

Table IV Mechanical Properties of Alloy 3 after Specified Heat Treatment

Heat Treat	Tensile Test Results					Stress Rupture Test Results				
	Temp °C	Yield MPa	Ult MPa	El %	RA %	Temp °C	Stress MPa	Time hr	El %	RA %
A	25	1110	1490	18.5	33.0	700	638	9.5	19.3	43.4
	25	1150	1535	17.5	31.4	700	638	13.9	22.6	44.6
	700	905	1035	25.2	35.0	700	638	23.3	10.6	14.6
B	700	940	1060	24.5	59.0					
	25	1225	1525	16.5	31.0	700	638	22.3	33.5	50.5
	25	1155	1510	17.0	31.0	700	638	17.4	25.0	42.2
	700	940	1055	28.0	63.5					
C	700	940	1055	28.0	63.5					
	25	1180	1525	14.5	29.0	700	638	8.7	32.9	49.3
	25	1160	1500	15.0	28.0	700	638	10.2	19.8	40.3
	700	975	1070	23.0	62.5					
	700	930	1035	38.5	64.0					

A = As heat treated      B = A + 700°C, 500 hr      C = A + 700°C, 1000 hr

should be noted that the results for Alloy 7 obtained with the new heat treatment are not much different than those obtained with the prior heat treatment.<sup>1</sup> Also, the present results confirm the initial results for Alloys 5 and 3.

Table V Average Tensile Test Results for Specified Heat Treatments

Alloy	Heat Treat	Temp °C	Yield MPa	Ult MPa	Elong %	RA %
5	A	25	1115	1473	21.7	35.1
		700	925	1140	9.9	16.1
	B	25	1123	1498	18.3	31.5
		700	1028	1155	31.0	34.5
	C	25	1190	1520	16.5	27.5
		700	1025	1160	25.0	46.2
7	A	25	1068	1478	20.5	29.2
		700	900	1115	10.5	14.5
	B	25	1065	1473	18.0	32.5
		700	980	1115	24.8	39.5
	C	25	1093	1483	17.5	28.8
		700	975	1093	26.3	35.7
3	A	25	1130	1513	18.0	32.2
		700	905	1035	25.2	35.0
	B	25	1190	1518	17.0	31.0
		700	940	1058	26.3	61.0
	C	25	1170	1513	14.7	28.5
		700	953	1053	30.8	63.3

A = As heat treated    B = A + 700°C, 500 hr    C = A + 700°C, 1000 hr

For comparison purposes, the average values from the tensile tests are listed in Table V. The results for Alloy 5 at 25°C and at 700°C continue to rise with length of exposure at 700°C while those for Alloys 3 and 7 remain essentially the same. The difference in stability properties (or sensitivity to temperature) becomes evident upon testing at 700°C after exposure to 1000 hr at 700°C. The respective yield and ultimate strength values are 1025 MPa (149 ksi) and 1160 MPa (168 ksi) for Alloy 5 compared to 975 MPa (142 ksi) and 1093 MPa (158 ksi) for Alloy 7. The values are even lower at 953 MPa (138 ksi) and 1053 MPa (153 ksi) for Alloy 3. Essentially the same differences are seen in a comparison of the results after the shorter 500 hr exposure at 700°C. Data in the literature for this type of testing have not been located except for the 1970 article on long time stability of Alloy 718 by Barker et al.<sup>15</sup> From production-scale ingot, pressed to billet and then upset-forged to pancake from which test bars were taken from tangential orientations, tensile test results at 650°C after 1000 hr exposure at 700°C were 745 MPa (108 ksi) yield and 1010 MPa (145 ksi) ultimate strength. It is evident in this oblique (indirect) comparison that all three modified 718 alloys have superior thermal stability properties compared to 1970 vintage 718 even when tensile tested at 50°C higher temperature.

Because turbine disk burst (the designer's primary concern) is by overspeed wherein the ultimate strength is approached by the average tangential stress, actual tensile properties after long-time service (exposure) are more important than hardness measurements. However, indentation hardness has been shown to be an indicator of the yield strength of a material. The average hardness as heat treated and then after 1000 hr at 700°C was RC 48.0 and RC 48.1 for Alloy 5, RC 46.7 and RC 46.9 for Alloy 7, and RC 47.1 and RC 47.3 for Alloy 3. There was no decrease in the hardness of each alloy from this exposure. The relative significance of these average values is seen in a comparison with Andrieu's values<sup>5</sup> of VHN445 (Rc 45) for Alloy 7 and VHN425 (Rc 43) for Alloy 718 after 1000 hr exposure to 700°C.

In the prior study,<sup>1</sup> Alloy 5 had two or three times the rupture life of Alloy 7 and Alloy 3 at 700°C under a stress of 638 MPa (92.5 ksi) and at 730°C under a stress of 483 MPa (70 ksi). Also, the stress rupture life of Alloy 5 at 650°C under a stress of 686 MPa (99.5 ksi), increased almost three-fold compared to conventional Alloy 718, and the 100 hr rupture life was higher by 14 to 22°C (57 to 72°F). The present stress rupture data for 700°C and 638 MPa (92.5 ksi) are also listed in Tables II to IV. The rupture life in the as heat treated condition is best in Alloy 5, followed by Alloy 7 and then Alloy 3. The same order persists upon testing after 500 hr and after 1000 hr at 700°C. The stress rupture life of Alloy 5 for the three conditions remains essentially the same (which is indicative of the  $\gamma''$  phase stability) while the lives of Alloy 7 and Alloy 3 are shorter following 1000 hr of aging at 700°C. Also, the tensile strength of Alloy 5 both at 25°C and 700°C increased with aging time at 700°C while the change in tensile strength of Alloys 7 and 3 was not obvious.

In summary, the tensile and stress rupture properties of Alloy 5 are better than those obtained on Alloy 7 and Alloy 3 under the specified conditions. However, it should be recognized that the aging time of 1000 hr at 700°C is not long enough for the completion of the aging curve. In these comparisons, the improvement in rupture life of Alloy 5 can be attributed to the observed difference in the  $\gamma'/\gamma''$  precipitates plus the effect of the tungsten addition in strengthening both the  $\gamma$  matrix and the  $\gamma'+\gamma''$  phases. In addition, the formation of a small chain-like  $M_6C$  precipitate in Alloy 5 strengthened the grain boundaries and thereby contributed to the improvement in rupture life. These differences in microstructure are covered in the next section.

#### Coarsening Results

The microstructure of each alloy by SEM techniques is illustrated in Figures 1 to 3. In each case, the as heat treated condition is shown along with that observed after aging for 1000 hr at 700°C and then after stress rupture testing at 700°C under 638 MPa. The micrographs illustrate the morphology of the  $\delta$  phase and primary MC phase. The precipitation of the  $\gamma'$  and  $\gamma''$  could not be resolved by SEM and was established by TEM. As seen in Figure 1, Alloy 5 has greater amounts of  $M_6C$  phase in the grain boundaries with  $\delta$  phase also present but none

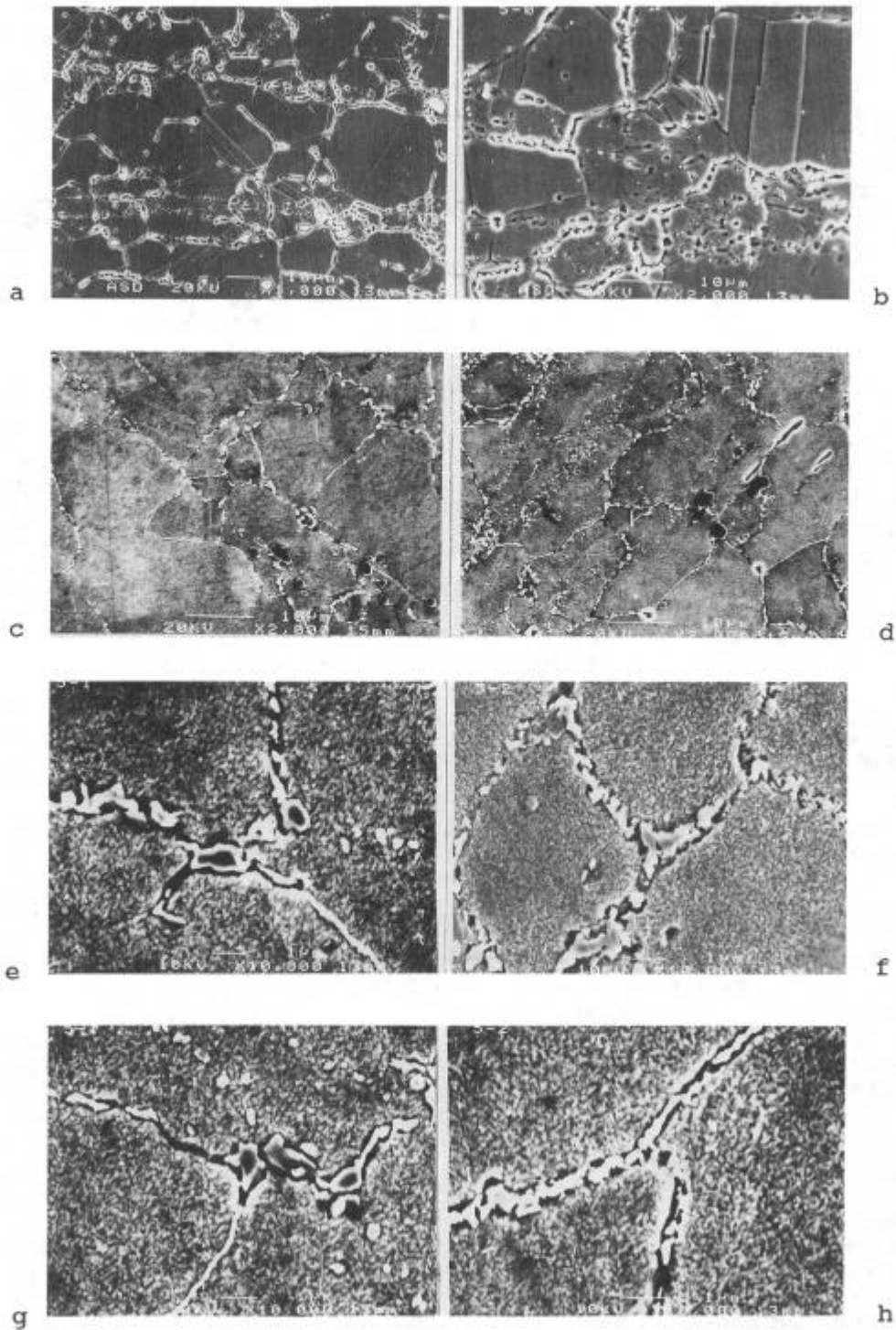


Figure 1 Scanning electron micrographs of Alloy 5. (a,b) After specific heat treatment. (c,e,g) After aging for 1000 hr at 700°C. (d,f,h) After stress rupture at 700°C and 638 MPa, 45.1 hr life.

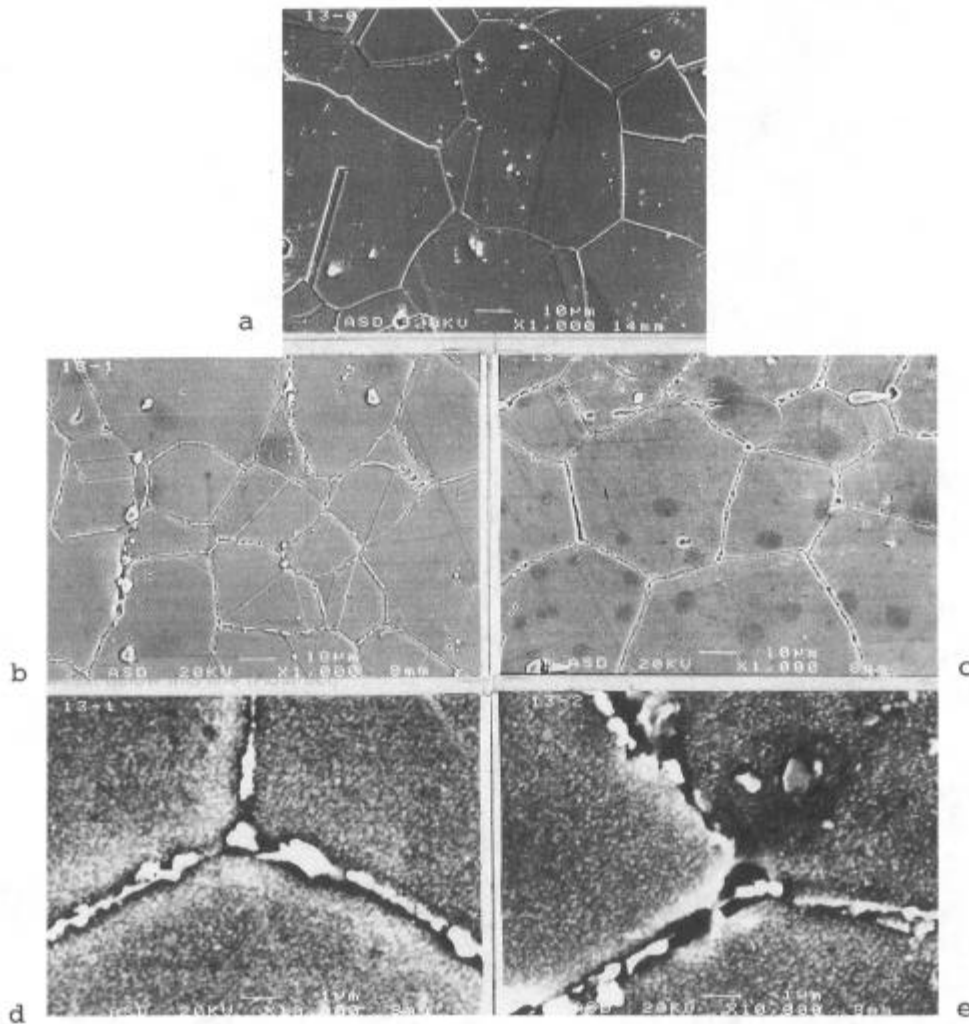


Figure 2 Scanning electron micrographs of Alloy 7. (a) After specific heat treatment. (b,d) After aging for 1000 hr at 700°C. (c,e) After stress rupture at 700°C and 638 MPa, 26 hr life.

within the grains for all three conditions. In Figure 2, the size and distribution of the  $\delta$  phase and its growth upon aging Alloy 7 for 1000 hr at 700°C is depicted. Again, there was no  $\delta$  phase precipitation within the grains. In the case of Alloy 3, a small amount of  $\delta$  phase of bar-like appearance was seen along with the usual increasing amount of  $\delta$  phase in the grain boundaries after aging for 1000 hr at 700°C, per Figure 3.

The prior heat treatment for Alloy 7 produced the distinctive compact  $\gamma'/\gamma''$  precipitate morphology shown in the initial study which had, for the heat treatment employed, a  $\gamma'$  size of about 0.033  $\mu\text{m}$  and  $\gamma''$  length about 0.023  $\mu\text{m}$ . A very small amount of  $\delta$  phase was seen in the grain boundaries but none intragrain. TEM micrographs of Alloy 7 for the new heat treatment employed in this study are shown in Figure 4. Again, it is seen that Alloy 7 has the compact  $\gamma'/\gamma''$  structure with  $\gamma'$  size measured as 0.021  $\mu\text{m}$  and  $\gamma''$  length at 0.012  $\mu\text{m}$ , which are much smaller than those obtained with the prior heat treatment. Hence,

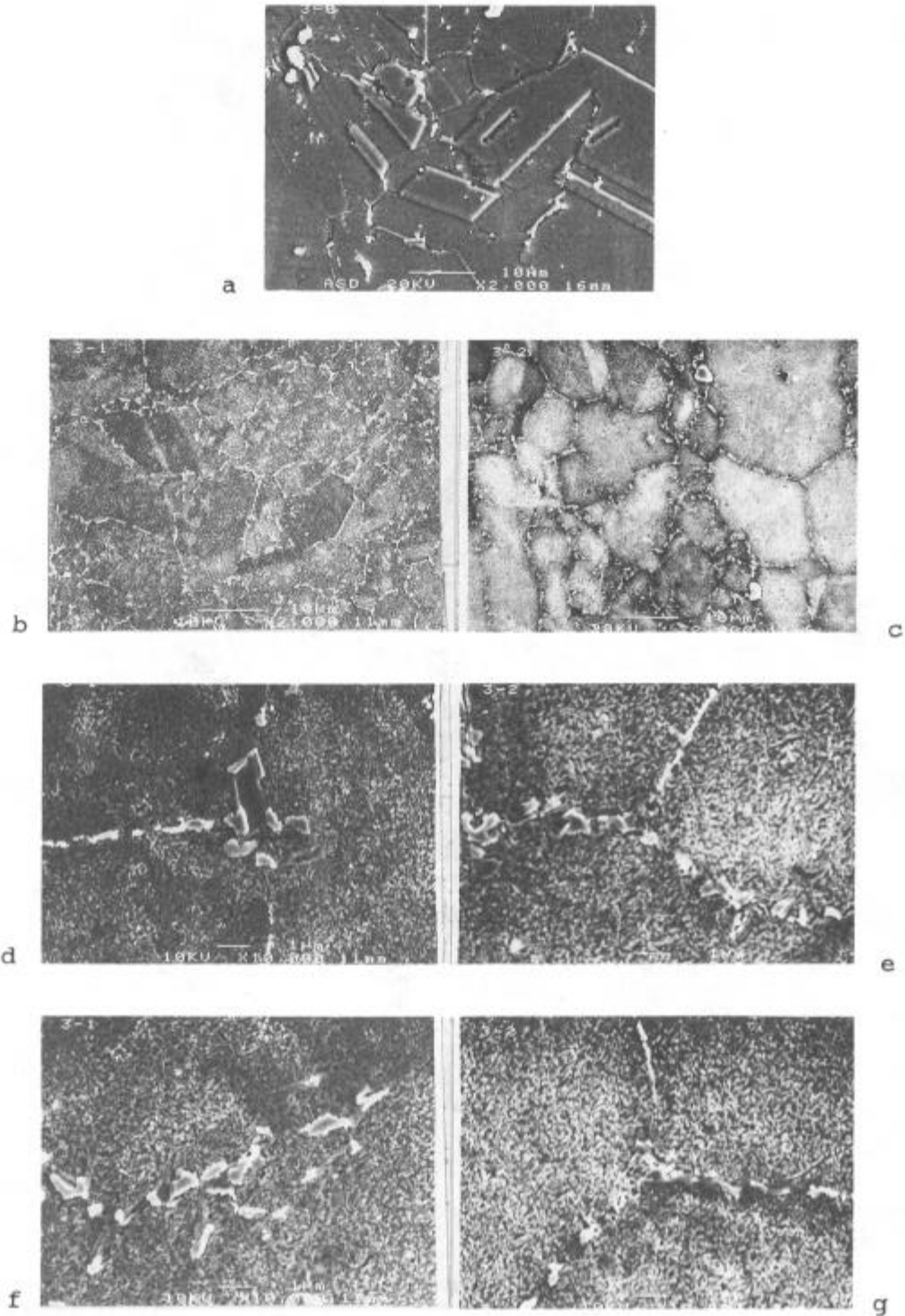


Figure 3 Scanning electron micrographs of Alloy 3. (a) After specific heat treatment. (b,d,f) After aging for 1000 hr at 700°C. (c,e,g) After stress rupture at 700°C and 638 MPa, 8.7 hr life.



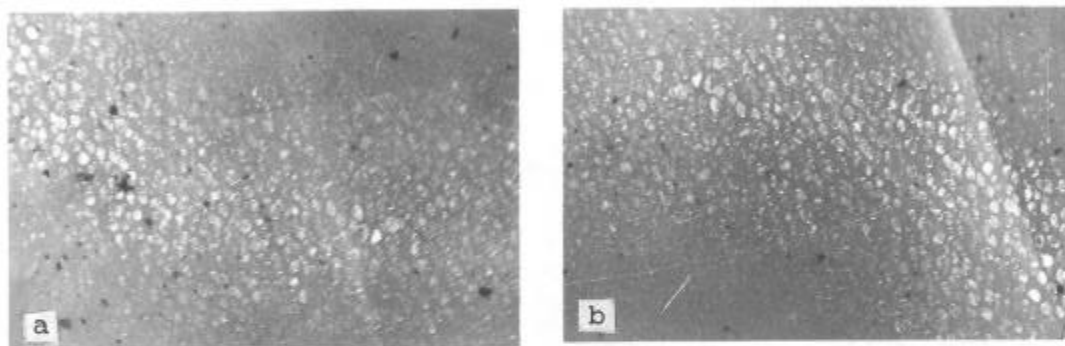


Figure 4 Transmission electron micrographs of Alloy 7 after specified heat treatment. (a,b) x 60000.

improved mechanical properties would be expected. Also, a very small amount of  $\delta$  phase was observed in the grain boundaries but none was seen intragrain. The TEM observations verified the SEM observations, per Figure 2.

TEM dark and bright field images for the three heat treated alloys subjected to 1000 hr aging at 700°C are depicted in Figure 5. The morphology of the  $\gamma'$  and  $\gamma''$  phases and the dimensional changes or coarsening (growth) rate after this aging (exposure) treatment will be described separately for each alloy.

Upon aging for 1000 hr at 700°C, Alloy 7 still has the compact  $\gamma'/\gamma''$  four-corner shape, per Figure 5. The  $\gamma''$  phase grew in sufficient length to envelope the  $\gamma'$  phase; so  $\gamma'$ 's size =  $\gamma''$  length = 0.032  $\mu\text{m}$ . This is an appreciable increase over the as heat treated measurements and closely similar to those measured after the heat treatment used in the previous study.<sup>1</sup> The growth rate of  $\gamma'$  and  $\gamma''$  in Alloy 7 was calculated as  $1.1 \times 10^{-5}$   $\mu\text{m/hr}$  for the  $\gamma'$  phase and  $2.0 \times 10^{-5}$   $\mu\text{m/hr}$  for the  $\gamma''$  phase. A greater amount of  $\delta$  phase was observed in the grain boundaries but there was no  $\delta$  phase within the grains which verifies the SEM observations, per Figure 2.

As shown in the prior study,<sup>1</sup> Alloy 5 has the non-compact  $\gamma'/\gamma''$  precipitate morphology with a mixture of disk-shaped  $\gamma''$  and hemispherical and partially four corner-shaped  $\gamma'$  particles, per Figure 6. The  $\gamma'$  size grew from 0.018  $\mu\text{m}$  to 0.026  $\mu\text{m}$  and the  $\gamma''$  length grew from 0.025  $\mu\text{m}$  to 0.032  $\mu\text{m}$ . The growth or coarsening rate was calculated as  $8 \times 10^{-6}$   $\mu\text{m/hr}$  for the  $\gamma'$  phase and  $7 \times 10^{-6}$   $\mu\text{m/hr}$  for the  $\gamma''$  phase. The coarsening rates after 1000 hr at 700°C are much slower in Alloy 5 compared to Alloy 7 (by an order of magnitude). More  $M_6C$  phase was observed in the grain boundaries but there was no  $\delta$  phase within the grains, which verified the SEM observations per Figure 1.

After aging for 1000 hr at 700°C, Alloy 3 revealed a non-compact  $\gamma'/\gamma''$  structure via TEM with the  $\gamma'$  phase being hemispherical and partially four-cornered shape while the  $\gamma''$

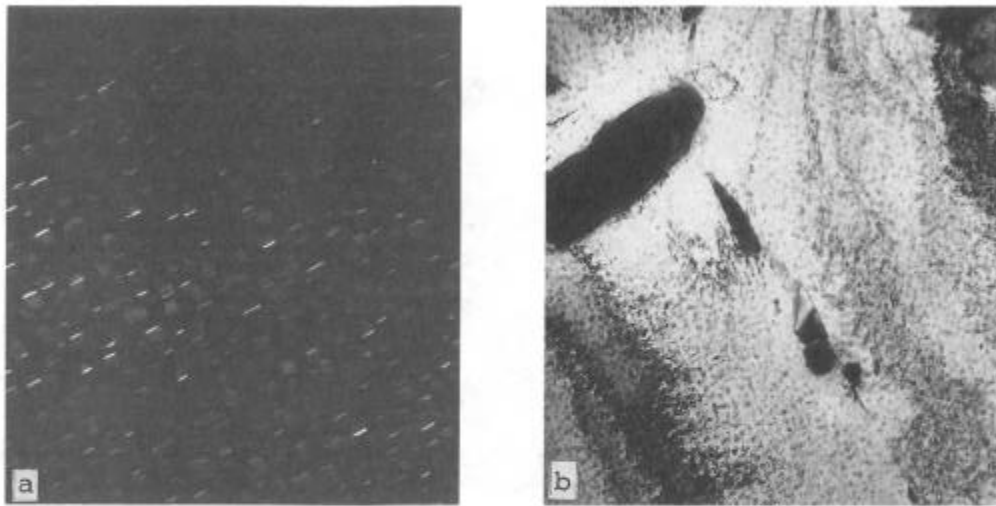


Figure 5 Transmission electron micrographs of Alloy 7 after heat treatment and aging for 1000 hr at 700°C. (a) x 60000. (b) x 17000.

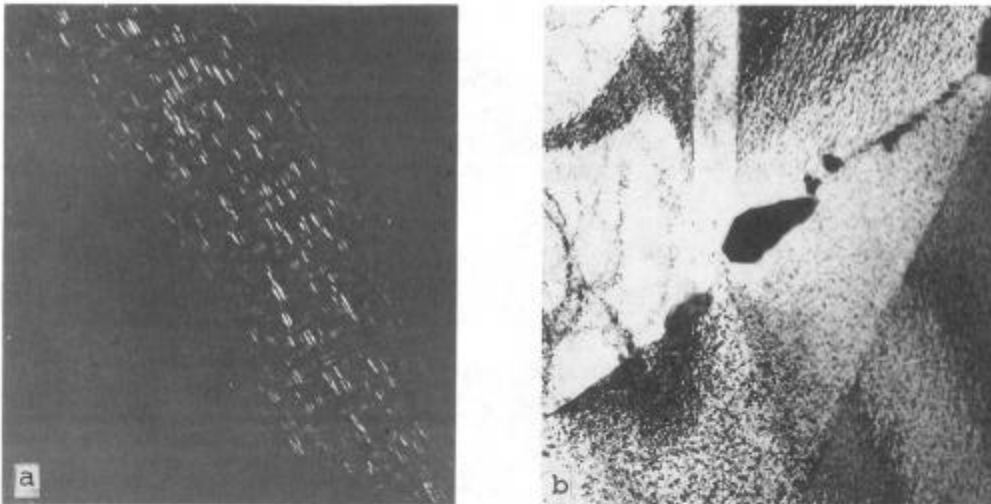


Figure 6 Transmission electron micrographs of Alloy 5 after heat treatment and aging for 1000 hr at 700°C. (a) x 60000. (b) x 17000.

phase was disk shaped, per Figure 7. As heat treated and reported in the prior study.<sup>1</sup> Alloy 3 had the compact  $\gamma'/\gamma''$  structure, with the  $\gamma'$  diameter and  $\gamma''$  length both measured at 0.038  $\mu\text{m}$ . After the aging treatment,  $\gamma'$  size was measured as 0.046  $\mu\text{m}$  and  $\gamma''$  length at 0.052  $\mu\text{m}$ . Hence, the growth rate was  $8 \times 10^{-6}$   $\mu\text{m/hr}$  for the  $\gamma'$  phase and  $1.4 \times 10^{-5}$   $\mu\text{m/hr}$  for the  $\gamma''$  phase. The coarsening rate of the  $\gamma'$  phase in Alloy 3 is the same as that measured in Alloy 5 but the rate for the  $\gamma''$  phase is significantly higher in this comparison. Both values were significantly lower when compared to the calculated values for Alloy 7. More  $\delta$  phase was observed in the grain boundaries with

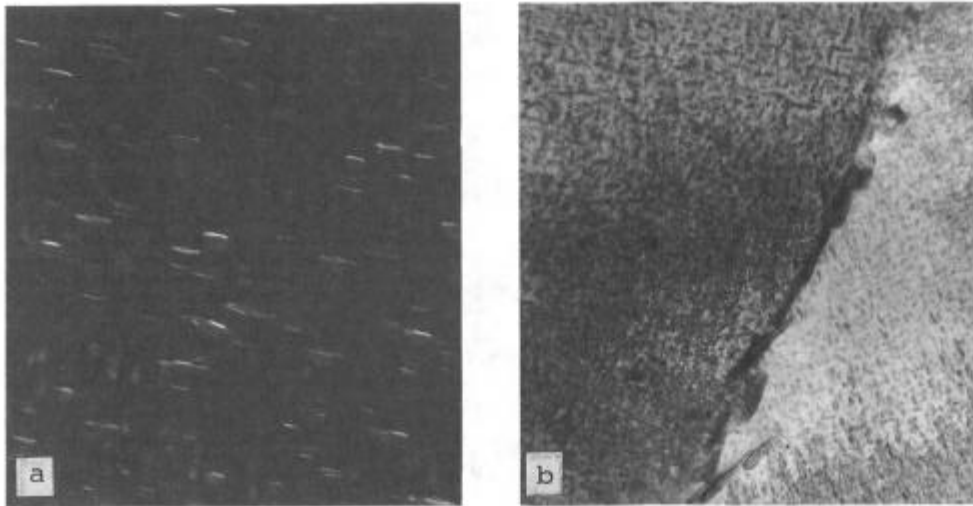


Figure 7 Transmission electron micrographs of Alloy 3 after heat treatment and aging for 1000 hr at 700°C. (a) x 60000. (b) x 17000.

a small amount of bar-shaped  $\delta$  phase observed within the grains, the TEM confirming the SEM, per Figure 3. The change in the  $\gamma'/\gamma''$  precipitate morphology after the 1000 hr exposure to 700°C caused the decrease in stress rupture life shown in Table IV.

The increase in precipitate size, after stress rupture testing at 700°C and 638 MPa the three alloys that were aged for 1000 hr at 700°C, is discussed in connection with Figures 8 and 9. Very little is known about the stress-enhanced coarsening rate effect and the data presented contribute to the scant information in the literature. Further work is needed to conclude more

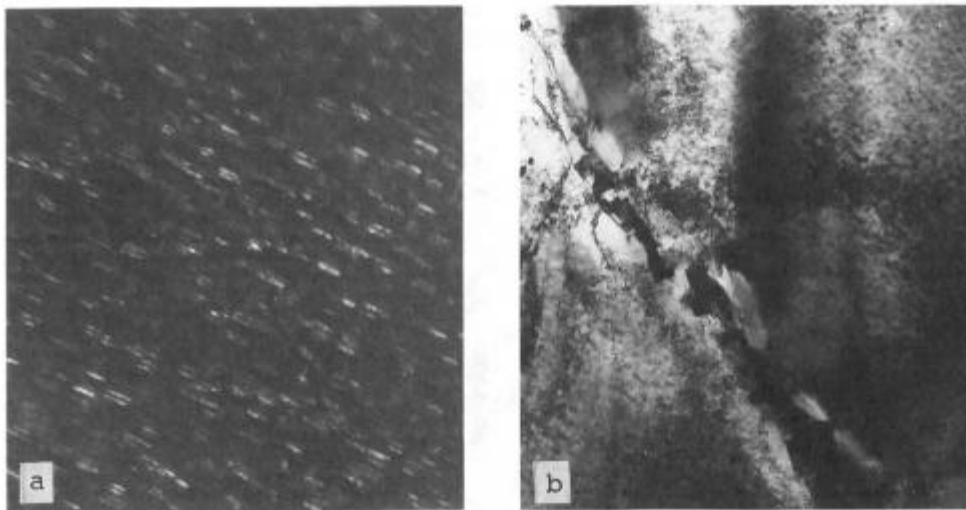


Figure 8 Transmission electron micrographs of Alloy 5 after heat treatment, aging for 1000 hr at 700°C and stress rupture at 700°C and 638 MPa. (a) x 60000. (b) x 17000.

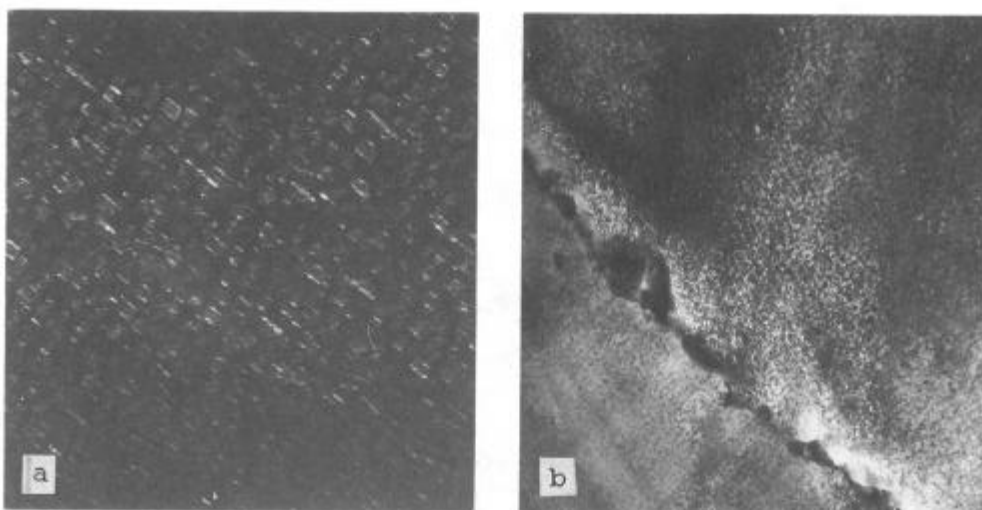


Figure 9 Transmission electron micrographs of Alloy 7 after heat treatment, aging for 1000 hr at 700°C and stress rupture at 700°C and 638 MPa. (a) x 60000. (b) x 17000.

quantitatively on the stress-enhanced coarsening behavior of Alloy 718 and its modifications. Of course, in examining the microstructures after stress rupture testing, it was recognized that there would be internal stress, dislocations and slip bands in the TEM foils.

As shown in Figure 8, Alloy 5 still has the non-compact  $\gamma'/\gamma''$  structure but there was some four-cornered  $\gamma'$  observed along with the hemisphere-shaped  $\gamma'$  phase.<sup>16</sup> The  $\gamma'$  size was measured at 0.038  $\mu\text{m}$  and  $\gamma''$  length at 0.040  $\mu\text{m}$ . The growth rate at 700°C under 637 MPa was calculated as  $2.6 \times 10^{-4}$   $\mu\text{m/hr}$  for the  $\gamma'$  phase and  $1.8 \times 10^{-4}$   $\mu\text{m/hr}$  for the  $\gamma''$  phase. More of the  $\text{M}_6\text{C}$  phase was

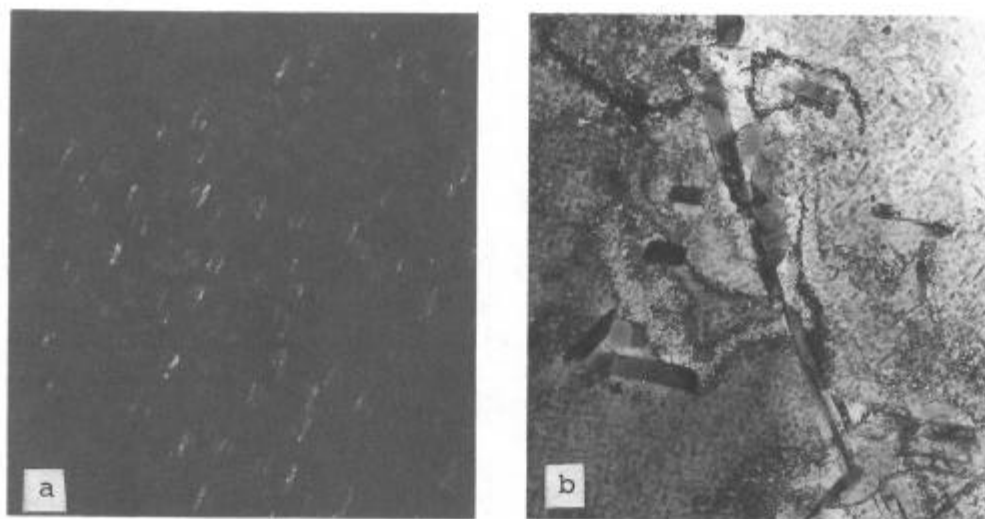


Figure 10 Transmission electron micrographs of Alloy 3 after heat treatment, aging for 1000 hr at 700°C and stress rupture at 700°C and 638 MPa. (a) x 60000. (b) x 17000.

observed in the grain boundaries but there was no  $\delta$  phase within the grains via TEM which confirmed the SEM views, per Figure 1.

Upon aging for 1000 hr at 700°C and stress rupture testing at 700°C under 637 MPa, Alloy 7 still has the four-cornered  $\gamma'/\gamma''$  compact structure, per Figure 9. The  $\gamma'$  size =  $\gamma''$  length = 0.038  $\mu\text{m}$ . The growth rate for both the  $\gamma'$  and  $\gamma''$  phase was calculated at  $2.3 \times 10^{-4}$   $\mu\text{m/hr}$ . Greater amounts of  $\delta$  phase was observed in the grain boundaries but there was none within the grains, again the TEM verified the SEM views, per Figure 2.

Under the testing conditions, Alloy 3 repeated its non-compact  $\gamma'/\gamma''$  structure with the  $\gamma'$  shape being hemispherical with partial four-cornered  $\gamma'$  phase, per Figure 10. The  $\gamma'$  size was measured at 0.051  $\mu\text{m}$  and  $\gamma''$  length at 0.057  $\mu\text{m}$ . The growth rate for both  $\gamma'$  and  $\gamma''$  was calculated as  $5.7 \times 10^{-4}$   $\mu\text{m/hr}$ . A greater amount of  $\delta$  phase was observed in the grain boundaries along with a small amount of  $\delta$  phase having a bar like appearance within the grain which was seen in both the TEM and SEM views, per Figure 3.

### Conclusions

In this continuation of our study comparing  $\gamma'/\gamma''$  precipitates and mechanical properties of three modified 718 alloys, emphasis was placed on their stability after aging for 500 and 1000 hr at 700°C. A major consideration was the comparison of the best alloy having a non-compact  $\gamma'/\gamma''$  precipitate structure with the specifically designed alloy that produced the cube-shaped, compact  $\gamma'/\gamma''$  precipitate. All three modifications produced superior tensile and stress rupture properties at 25°C and 700°C when compared to conventional Alloy 718. The results obtained with the non-compact  $\gamma'/\gamma''$  precipitate were better than those obtained with the compact  $\gamma'/\gamma''$  precipitate upon aging for 1000 hr at 700°C. The improvement in properties is attributed to the difference in coarsening behavior of the two precipitate morphologies plus the effect of a tungsten addition in strengthening both the  $\gamma$  matrix and the  $\gamma'+\gamma''$  phases. In addition, the formation of a small chain-like  $\text{M}_6\text{C}$  strengthened the grain boundaries and thereby contributed to the improvement in rupture life. As heat treated, the  $\gamma'$  precipitate size was smaller in the alloy having the non-compact  $\gamma'/\gamma''$  precipitate morphology. The coarsening (growth) rate of the  $\gamma'$  and  $\gamma''$  particles after aging for 1000 hr at 700°C and after stress rupture testing at 700°C and 638 MPa (92.5 ksi) following this exposure was less in the alloy having the non-compact  $\gamma'/\gamma''$  precipitate compared to the alloy having the compact  $\gamma'/\gamma''$  precipitate, as well as the third alloy which changed from a cube-shape to a mixture of basically non-compact  $\gamma'/\gamma''$  precipitate after these thermal treatments.

### References

1. E. Guo, F. Xu and E.A. Loria, Superalloys 718, 625 and Various Derivatives, TMS (1991), pp. 397-408.
2. E. Guo, F. Xu and E.A. Loria, Superalloy 718: Metallurgy and Applications, TMS (1989), pp. 567-576.

3. E. Guo, F. Xu and E.A. Loria, Superalloys 718, 625 and Various Derivatives, TMS (1991), pp. 389-396.
4. E.A. Loria, High Temperature Materials for Power Engineering 1990, CRM Liege, Kluwer Academic Publishers (1990), pp. 1367-1375.
5. E.A. Loria, JOM, TMS (June 1992), pp. 33-36.
6. J.P. Collier, S.H. Wong, J.C. Phillips and J. K. Tien, Metall. Trans., 19A (1988), pp. 1657-1666.
7. J.P. Collier, A.O. Selius and J.K. Tien, Superalloys 88, TMS (1988), pp. 43-52.
8. J.K. Tien, J.P. Collier, P.L. Bretz and B.C. Hendrix, High Temperature Materials for Power Engineering 1990, CRM Liege, Kluwer Academic Publishers (1990), pp. 1341-1356.
9. J.A. Manriquez, P.L. Bretz, L. Rabenberg and J.K. Tien, Superalloys 1992, TMS (1992), pp. 507-516.
10. E. Andrieu, R. Cozar and A. Pineau, Superalloy 718: Metallurgy and Applications, TMS (1989), pp. 241-256.
11. E. Andrieu, private communication (September 1991).
12. E. Andrieu and A. Pineau, Paper in this volume.
13. Xishan Xie et al, Paper in this volume.
14. K-M. Chang, US Patent 4981644, January 1, 1991, 20 pp.
15. J. F. Barker, E.W. Ross and J.F. Radavich, Journal of Metals, TMS (January 1970), pp. 31-41.
16. M. Sundararaman, P. Mukhopadhyay and S. Banerjee, Metall. Trans., 23A (1992), pp. 2015-2028.